The 9th European Congress on Computational Methods in Applied Sciences and Engineering
ECCOMAS Congress 2024
3–7 June 2024, Lisboa, Portugal

FINITE ELEMENT FORMULATIONS FOR AXISYMMETRIC SOLIDS: A NEW APPROACH BASED ON THE PETROV-GALERKIN METHOD

FELIX ZÄHRINGER[1] AND PETER BETSCH[1]

[1] Institute of Mechanics
Karlsruhe Institute of Technology
Otto-Ammann-Platz 9, 76131 Karlsruhe, Germany
e-mail: felix.zaehringer@kit.edu, www.ifm.kit.edu

Key words: Finite Element Method, Petrov-Galerkin, Axisymmetric Solids, Mesh Sensitivity

Summary. The sensitivity of conventional finite element formulations to distorted meshes is a well-known problem. In this work, it is investigated whether an 8-node Petrov-Galerkin finite element formulation can reduce this mesh-sensitive behavior when simulating linear-elastic axisymmetric problems. The numerical investigations show that the Petrov-Galerkin formulation exhibits significantly better behavior than the Bubnov-Galerkin formulation in certain cases. However, the results also indicate that this is not generally the case.

1 INTRODUCTION

The simulation of problems in solid mechanics is commonly done today using the finite element method. Over time, a wide range of element formulations has been developed for different classes of problems. The problem class of axisymmetric solids is in the focus of this work. This class is characterized by specific features that will be explained in more detail in the following sections. It is important to note that these particular features often prevent solution strategies from other problem classes from being transferred to axisymmetric problems. The central motivation of this work is therefore to investigate whether the core ideas of Petrov-Galerkin finite element formulations for plane solids can be applied to these axisymmetric problems.

It is well known that conventional finite element formulations react sensitively to the use of meshes with distorted elements [1]. More precisely, with the same number of elements and the same approximation order, mesh distortion leads to a significant decline in approximation accuracy. This effect can also be observed when simulating axisymmetric solids.

With the intention of reducing this mesh sensitivity for plane problems, Rajendran and Liew [2] developed an 8-node Petrov-Galerkin finite element formulation. Petrov-Galerkin formulations are characterized by the fact that the virtual displacement field and the displacement field are approximated using different shape functions. This is in contrast to conventional Bubnov-Galerkin finite element formulations, in which the virtual displacement field and the displacement field are approximated using the same shape functions.

In Rajendran and Liew's formulation [2], the virtual displacement field is approximated using the well-established quadratic Serendipity shape functions, while the displacement field is approximated with so-called metric shape functions. These metric shape functions are specifically designed to accurately reproduce quadratic displacement fields, even in the presence of distorted

element geometries. For comparison: Conventional quadratic Serendipity shape functions only achieve this when using regular meshes.

Since the metric shape functions were originally defined depending on the physical coordinates, the shape functions were not independent of superposed rigid body motions and thus frame-dependent. To solve this problem, Xie et al. [3] proposed to define the metric shape functions depending on skew coordinates instead. This idea solved the problem of frame dependency while at the same time preserving the ability to accurately reproduce quadratic displacement fields for highly distorted element geometries.

In this work, it is investigated whether the concepts from these works can be transferred to axisymmetric problems. More precisely, it is examined whether a Petrov-Galerkin finite element formulation has advantages in terms of mesh sensitivity compared to the standard Bubnov-Galerkin formulation when simulating axisymmetric problems.

2 THE BOUNDARY VALUE PROBLEM OF AXISYMMETRIC SOLIDS

As mentioned in the introduction, this article addresses a special class of problems within the field of solid mechanics, namely axisymmetric problems. Specifically, these are three-dimensional structures that are symmetric with respect to an axis of revolution. The symmetry refers not only to the geometry of the structure, but also to its loading and boundary conditions. These problems can be described using a cylindrical coordinate system, as illustrated in Figure 1. This section briefly summarizes the most important relationships; further details can be found in standard references [4, 5].

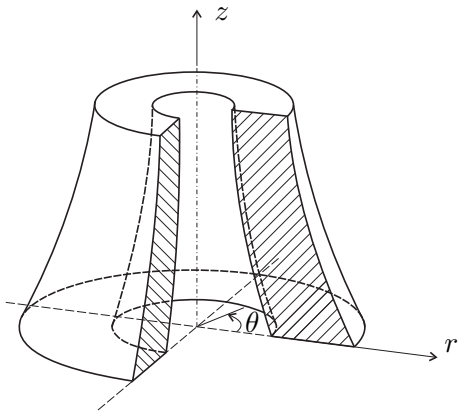

Figure 1: Illustration of an axisymmetric problem with a cylindrical coordinate system.

Due to the symmetry, it is sufficient to consider a plane section of the body, e.g., the r-z plane. The displacement vector can then be expressed as

$$\mathbf{u} = \begin{bmatrix} u \\ w \end{bmatrix}, \tag{1}$$

where u and w are the displacements in the r- and z-direction, respectively.

The strain tensor has four non-zero entries for axisymmetric problems, which can be arranged compactly in a vector, namely as

$$\boldsymbol{\varepsilon} = \begin{bmatrix} \varepsilon_r \\ \varepsilon_z \\ \gamma_{rz} \\ \varepsilon_\theta \end{bmatrix} = \begin{bmatrix} \partial u/\partial r \\ \partial w/\partial z \\ \partial u/\partial z + \partial w/\partial r \\ u/r \end{bmatrix}. \tag{2}$$

In the case of isotropic linear elastic material behavior, the stresses can be calculated using

$$\boldsymbol{\sigma} = \begin{bmatrix} \sigma_r \\ \sigma_z \\ \tau_{rz} \\ \sigma_\theta \end{bmatrix} = \mathbf{C}\,\boldsymbol{\varepsilon}, \tag{3}$$

where the associated elasticity matrix has the form

$$\mathbf{C} = \begin{bmatrix} 1-\nu & \nu & 0 & \nu \\ \nu & 1-\nu & 0 & \nu \\ 0 & 0 & \frac{1-2\nu}{2} & 0 \\ \nu & \nu & 0 & 1-\nu \end{bmatrix}. \tag{4}$$

To be able to compute axisymmetric problems using the finite element method, the corresponding weak form is required. Using the principle of minimum potential energy, the equation to be discretized is obtained as

$$\delta W = \delta W_{\text{int}} + \delta W_{\text{ext}} = 0, \tag{5}$$

where

$$\delta W_{\text{int}} = 2\pi \int_\Omega \delta\boldsymbol{\varepsilon}^{\mathrm{T}}\, \mathbf{C}\, \boldsymbol{\varepsilon}\, r \, \mathrm{d}r\, \mathrm{d}z \tag{6}$$

and

$$\delta W_{\text{ext}} = -2\pi \left(\int_\Omega \delta\mathbf{u}^{\mathrm{T}}\, \mathbf{b}\, r \, \mathrm{d}r\, \mathrm{d}z + \int_{\partial\Omega_N} \delta\mathbf{u}^{\mathrm{T}}\, \bar{\mathbf{t}}\, r \, \mathrm{d}s \right). \tag{7}$$

Following the usual notation, $\delta\mathbf{u}$ denotes the virtual displacement vector. Furthermore, $\mathbf{b}$ is a distributed body force and $\bar{\mathbf{t}}$ denotes given tensions on the Neumann boundary $\partial\Omega_N$.

It is evident that there are two major differences between finite element formulations for axisymmetric problems and those for plane problems. Firstly, both the strain vector (2) and the stress vector (3) have an additional entry to account for the strain or stress in the circumferential direction. Secondly, the radius r appears in the integrands of Equations (6) and (7), and consequently also affects the stiffness matrix and the load vector after discretization.

These differences present a challenge for transferring, for example, mixed finite element formulations from plane to axisymmetric problems (cf. e.g. [6]). The main motivation of this study is therefore to investigate whether these differences also pose an obstacle to using the Petrov-Galerkin finite element method in the context of axisymmetric problems.

3 8-NODE PETROV-GALERKIN FINITE ELEMENT FORMULATION

In this section, the 8-node Petrov-Galerkin finite element formulation for the simulation of axisymmetric problems is briefly introduced. This formulation is based on two Petrov-Galerkin finite element formulations for the simulation of plane problems [2, 3].

3.1 Approximation of the geometry and the virtual displacement field

Exactly as in Bubnov-Galerkin finite element formulations, the geometry is approximated by

$$r^{\mathrm{h},e} = \sum_{i=1}^{8} N_i(\boldsymbol{\xi})\, r_i^e, \qquad z^{\mathrm{h},e} = \sum_{i=1}^{8} N_i(\boldsymbol{\xi})\, z_i^e \tag{8}$$

for the Petrov-Galerkin finite element formulation. Therein, N_i are the well-established quadratic Serendipity shape functions (cf. [5]). The virtual displacement field is approximated analogously via

$$\delta\mathbf{u}^{\mathrm{h},e} = \sum_{i=1}^{8} N_i(\boldsymbol{\xi})\, \delta\mathbf{u}_i^e. \tag{9}$$

This choice ensures that all continuity requirements are satisfied (cf. [2]).

3.2 Approximation of the displacement field

The displacement field is not approximated using Serendipity shape functions. Instead, so-called metric shape functions are employed. A key difference is that these metric shape functions are not constructed in the reference element based on the natural coordinates ξ and η, but instead in an intermediate configuration based on the skew coordinates $\bar{\xi}$ and $\bar{\eta}$ (see Figure 2).

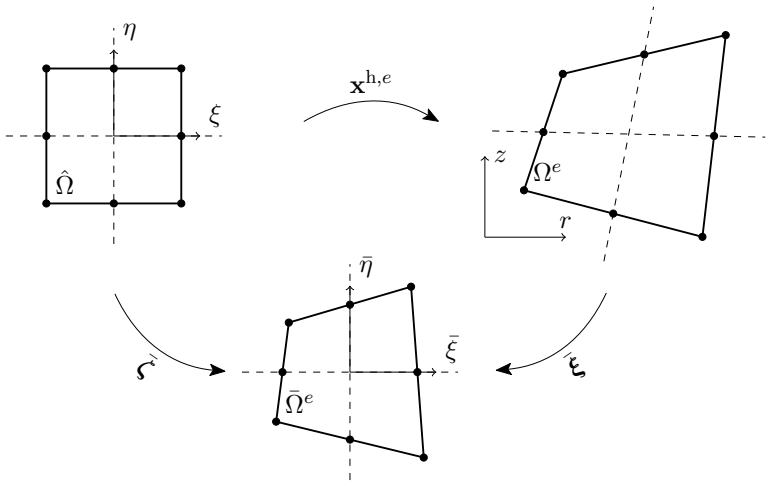

Figure 2: Illustration of the reference element $\hat{\Omega}$, the skew element $\bar{\Omega}^e$, and the physical element Ω^e with their respective coordinate systems.

The skew coordinates are defined by

$$\bar{\boldsymbol{\xi}} = \begin{bmatrix} \bar{\xi} \\ \bar{\eta} \end{bmatrix} = \left(\mathbf{J}\Big|_{\boldsymbol{\xi}=0} \right)^{-1} \left(\begin{bmatrix} r^{\mathrm{h},e} \\ z^{\mathrm{h},e} \end{bmatrix} - \begin{bmatrix} r^{\mathrm{h},e} \\ z^{\mathrm{h},e} \end{bmatrix} \Big|_{\boldsymbol{\xi}=0} \right), \tag{10}$$

where $\mathbf{J}$ is the Jacobian matrix. This definition for axisymmetric problems is in accordance with the original definition for plane problems [7] and allows an affine transformation between the physical coordinates and the skew coordinates for each element.

The metric shape functions M_i^e are computed, following Xie et al. [3], elementwise via

$$\begin{bmatrix} M_1^e \\ M_2^e \\ M_3^e \\ M_4^e \\ M_5^e \\ M_6^e \\ M_7^e \\ M_8^e \end{bmatrix} = \begin{bmatrix} 1 & 1 & 1 & 1 & 1 & 1 & 1 & 1 \\ \bar{\xi}_1 & \bar{\xi}_2 & \bar{\xi}_3 & \bar{\xi}_4 & \bar{\xi}_5 & \bar{\xi}_6 & \bar{\xi}_7 & \bar{\xi}_8 \\ \bar{\eta}_1 & \bar{\eta}_2 & \bar{\eta}_3 & \bar{\eta}_4 & \bar{\eta}_5 & \bar{\eta}_6 & \bar{\eta}_7 & \bar{\eta}_8 \\ \bar{\xi}_1\bar{\eta}_1 & \bar{\xi}_2\bar{\eta}_2 & \bar{\xi}_3\bar{\eta}_3 & \bar{\xi}_4\bar{\eta}_4 & \bar{\xi}_5\bar{\eta}_5 & \bar{\xi}_6\bar{\eta}_6 & \bar{\xi}_7\bar{\eta}_7 & \bar{\xi}_8\bar{\eta}_8 \\ \bar{\xi}_1^2 & \bar{\xi}_2^2 & \bar{\xi}_3^2 & \bar{\xi}_4^2 & \bar{\xi}_5^2 & \bar{\xi}_6^2 & \bar{\xi}_7^2 & \bar{\xi}_8^2 \\ \bar{\eta}_1^2 & \bar{\eta}_2^2 & \bar{\eta}_3^2 & \bar{\eta}_4^2 & \bar{\eta}_5^2 & \bar{\eta}_6^2 & \bar{\eta}_7^2 & \bar{\eta}_8^2 \\ \bar{\xi}_1^2\bar{\eta}_1 & \bar{\xi}_2^2\bar{\eta}_2 & \bar{\xi}_3^2\bar{\eta}_3 & \bar{\xi}_4^2\bar{\eta}_4 & \bar{\xi}_5^2\bar{\eta}_5 & \bar{\xi}_6^2\bar{\eta}_6 & \bar{\xi}_7^2\bar{\eta}_7 & \bar{\xi}_8^2\bar{\eta}_8 \\ \bar{\xi}_1\bar{\eta}_1^2 & \bar{\xi}_2\bar{\eta}_2^2 & \bar{\xi}_3\bar{\eta}_3^2 & \bar{\xi}_4\bar{\eta}_4^2 & \bar{\xi}_5\bar{\eta}_5^2 & \bar{\xi}_6\bar{\eta}_6^2 & \bar{\xi}_7\bar{\eta}_7^2 & \bar{\xi}_8\bar{\eta}_8^2 \end{bmatrix}^{-1} \begin{bmatrix} 1 \\ \bar{\xi} \\ \bar{\eta} \\ \bar{\xi}\bar{\eta} \\ \bar{\xi}^2 \\ \bar{\eta}^2 \\ \bar{\xi}^2\bar{\eta} \\ \bar{\xi}\bar{\eta}^2 \end{bmatrix},$$

where $\bar{\xi}_i$ and $\bar{\eta}_i$ are the skew coordinates of node i.

The displacement field is then approximated by

$$\mathbf{u}^{\mathrm{h},e} = \sum_{i=1}^{8} M_i^e(\bar{\boldsymbol{\xi}})\, \mathbf{u}_i^e. \tag{11}$$

Approximating the displacement field in this way makes it possible to reproduce quadratic displacement fields exactly even in the presence of highly distorted meshes. The subsequent procedure does not deviate from the standard procedure in finite element methods and will therefore not be further elaborated.

4 NUMERICAL EXAMPLES

In this section, the Petrov-Galerkin finite element formulation is investigated using three numerical examples. The considered linear-elastic problems are all simulated using the same material parameters (Young's modulus $E = 1 \times 10^7$, Poisson's ratio $\nu = 0.3$). Furthermore, the 3×3 Gaussian quadrature rule is employed in all examples.

4.1 Circular plate subjected to pure bending

As a first example, a circular plate is considered which is subjected to a moment $\bar{m}$ at the edge of the plate (see Figure 3). For this axisymmetric problem, there exists an analytical solution for the vertical displacement

$$w = \frac{\bar{m}}{2(1+\nu)D}(R^2 - r^2), \tag{12}$$

which can be deduced from plate theory (cf. [8]). In the equation above,

$$D = \frac{E\, t^3}{12(1-\nu^2)}. \tag{13}$$

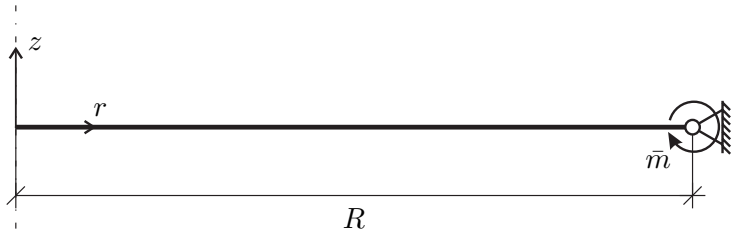

Figure 3: Illustration of the circular plate problem.

According to the considerations from Section 3, the 8-node Petrov-Galerkin element PG-Q8 should be able to reproduce this quadratic displacement function exactly even when highly distorted meshes are used. To verify this, the resulting vertical displacement w_{eval} at the point $(r,\, z) = (0,\, 0)$ is computed numerically. For the simulation it is assumed that $R = 10$ and $t = 1$. Moreover, the magnitude of the moment $\bar{m}$ is selected in such a way that an analytical solution $w_{\text{eval}} = 1$ is obtained.

The problem is discretized with two elements as shown in Figure 4. Various simulations are carried out, in which the mesh distortion parameter s is varied and thus different degrees of mesh distortion are tested.

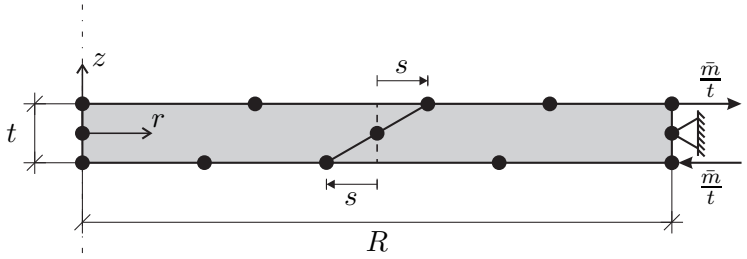

Figure 4: Discretization of the circular plate problem.

As can be seen from Table 1 and Figure 5, the 8-node Petrov-Galerkin element PG-Q8 is completely independent of the present mesh distortion. In contrast, the 8-node Bubnov-Galerkin element Q8 is significantly affected by the mesh distortion.

Table 1: Resulting vertical displacement w_{eval} for the circular plate example at $(r,\, z) = (0,\, 0)$ for different values of s.

	$s = 0$	$s = 1$	$s = 2$	$s = 3$	$s = 4$	$s = 4.5$
Q8	1.0000	0.9693	0.8042	0.7067	0.6735	0.6575
PG-Q8	1.0000	1.0000	1.0000	1.0000	1.0000	1.0000

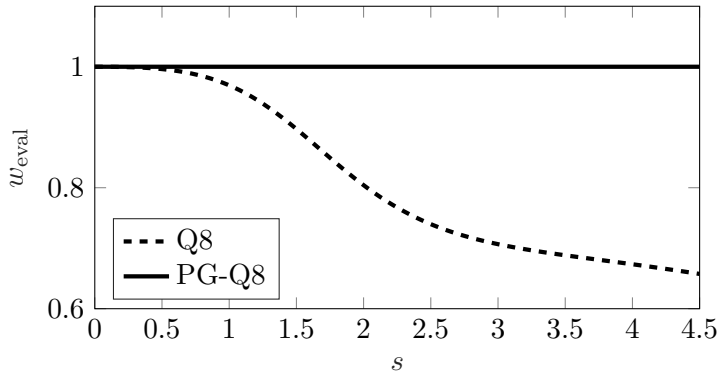

Figure 5: Illustration of the resulting vertical displacement w_{eval} for the circular plate example at $(r,\, z) = (0,\, 0)$ for different values of s.

4.2 Cylindrical shell subjected to a distributed body force

As a second example, a cylindrical shell subjected to a distributed body force $\mathbf{b} = \begin{bmatrix} 0, & b_z \end{bmatrix}^{\mathrm{T}}$ is considered. For this example, an analytical solution for the displacement field can be found based on the theory of cylindrical shells (see, e.g., [9]). More precisely, in this case, the displacement field of the shell's mid-surface is given by

$$u = -b_z \frac{\nu R}{Et} (h - z), \quad w = b_z \frac{h}{Et} \left(z - \frac{z^2}{2h} \right). \tag{14}$$

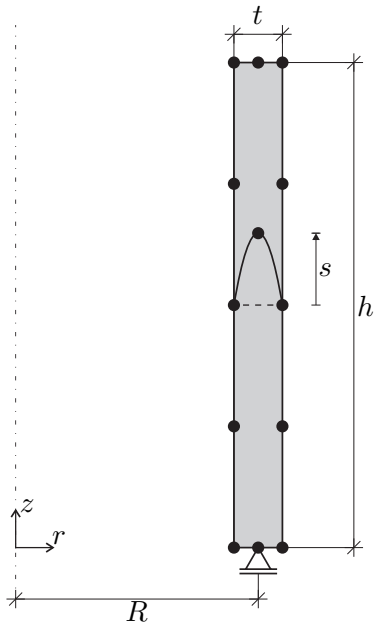

Figure 6: The system and discretization of the cylindrical shell example.

Since the displacement field once again involves only terms up to quadratic order, the Petrov-Galerkin 8-node element should be able to reproduce this displacement field exactly. To demonstrate this numerically, the problem is again discretized using two elements; however, this time, a curved-edge distortion is applied (see Figure 6). For the simulations, it is assumed that $R = 5$, $h = 10$, and $t = 1$. The radial displacement u_{eval} at the point $(r, z) = (R, 0)$ is measured. Similar to the first example, the magnitude of the body force b_z is chosen in such a way that according to (14) $u_{\text{eval}} = 1$. Furthermore, to prevent the occurrence of singularities due to the point support, a vertical pressure $p_z = -b_z h$ is applied in the simulations at the bottom of the cylinder to balance the body force.

Several simulations are performed again, varying the mesh distortion parameter s. From Table 2 and Figure 7, it is evident that the 8-node Petrov-Galerkin element PG-Q8 is capable of accurately reproducing the displacement field in this case as well, whereas the 8-node Bubnov-Galerkin element Q8 shows a strongly mesh-dependent behavior. Similar observations can be made when other evaluation points are chosen, or when the vertical displacement is measured instead of the radial displacement.

Table 2: Resulting radial displacement u_{eval} for the cylindrical shell example at $(r, z) = (R, 0)$ for different values of s.

	$s = 0$	$s = 1$	$s = 2$	$s = 3$	$s = 4$	$s = 4.5$
Q8	1.0000	0.9709	0.9037	0.8219	0.7353	0.6868
PG-Q8	1.0000	1.0000	1.0000	1.0000	1.0000	1.0000

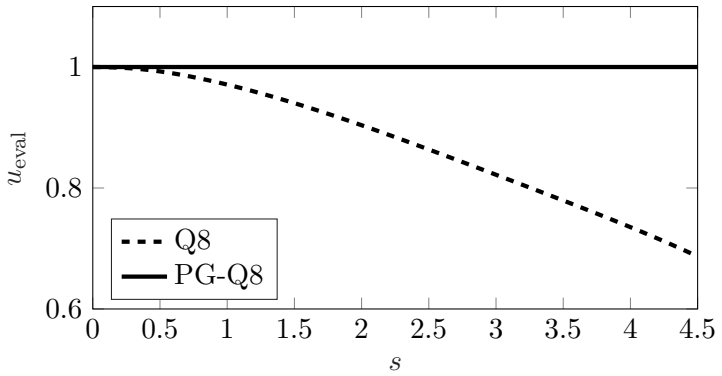

Figure 7: Illustration of the resulting radial displacement u_{eval} for the cylindrical shell example at $(r, z) = (R, 0)$ for different values of s.

4.3 Thick-walled cylinder under internal pressure

As a final example, a thick-walled cylinder under internal pressure is considered. For this problem, the analytical solution (see, e.g., [6]) for the radial displacement is given by

$$u = \frac{(1+\nu)\, p\, R_i^2}{E\,(R_o^2 - R_i^2)} \left(\frac{R_o^2}{r} + (1-2\nu)\, r \right), \tag{15}$$

where p is the magnitude of the pressure and R_i and R_o are the inner and the outer radius of the cylinder, respectively. The problem is illustrated in Figure 8.

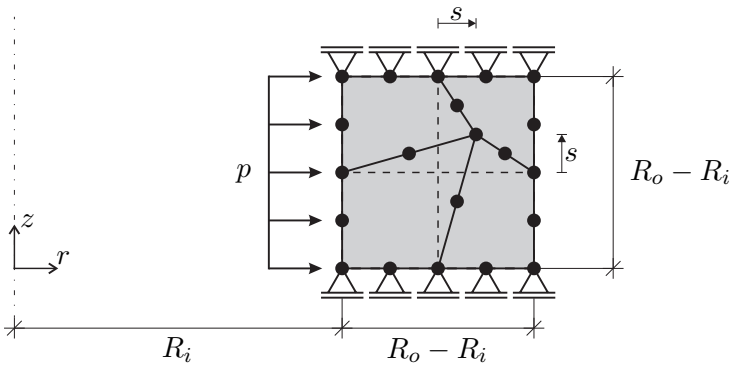

Figure 8: The system and discretization of the thick-walled cylinder example.

It can be seen that for this problem the displacement field is no longer a polynomial. Therefore, it can be expected that neither the 8-node Petrov-Galerkin element nor the 8-node Bubnov-Galerkin element can reproduce the displacement field exactly. To examine this example numerically, the radial displacement u_{eval} at point $(r,\, z) = (R_i,\, 0)$ is investigated. Similar to the other examples, the magnitude of the pressure p is selected in such a way that according to (15) $u_{\text{eval}} = 1$.

The problem is discretized with 4 elements as shown in Figure 8. To investigate the influence of mesh distortion, the center node is moved by a value s, as depicted.

First, the case that $R_i = 1$ and $R_o = 5$ is considered. The simulation results, which are shown in Table 3 and Figure 9, reveal the following. Firstly, as expected, it can be seen that none of the elements considered is able to reproduce the displacement field exactly. Secondly, both elements show a mesh-dependent behavior. Another remarkable fact is that, in this example, the Bubnov-Galerkin element Q8 provides a slightly better approximation of the displacement field than the Petrov-Galerkin element PG-Q8 when the mesh is distorted.

Table 3: Resulting radial displacement u_{eval} for the thick-walled cylinder example at $(r,\, z) = (R_i,\, 0)$ for different values of s. These values have been computed using $R_i = 1$ and $R_o = 5$.

	$s = 0$	$s = 0.15$	$s = 0.3$	$s = 0.45$	$s = 0.6$	$s = 0.75$	$s = 0.9$
Q8	0.9591	0.9554	0.9514	0.9470	0.9422	0.9370	0.9314
PG-Q8	0.9591	0.9553	0.9510	0.9462	0.9411	0.9356	0.9299

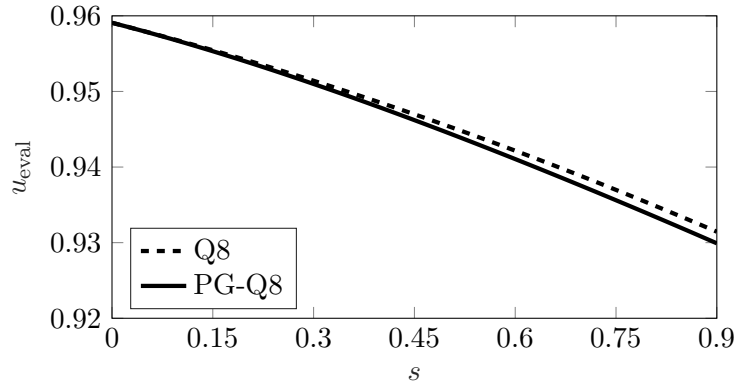

Figure 9: Illustration of the resulting radial displacement u_{eval} for the thick-walled cylinder example at $(r,\, z) = (R_i,\, 0)$ for different values of s. These values have been computed using $R_i = 1$ and $R_o = 5$.

If, on the other hand, $R_i = 1$ and $R_o = 2$ are selected as simulation parameters, the results shown in Table 4 and Figure 10 are obtained. Here it can be seen that the Petrov-Galerkin element PG-Q8 again provides a slightly better approximation than the Bubnov-Galerkin element Q8.

Table 4: Resulting radial displacement u_{eval} for the thick-walled cylinder example at $(r,\, z) = (R_i,\, 0)$ for different values of s. These values have been computed using $R_i = 1$ and $R_o = 2$.

	$s = 0$	$s = 0.05$	$s = 0.1$	$s = 0.15$	$s = 0.2$
Q8	0.9992	0.9990	0.9988	0.9985	0.9980
PG-Q8	0.9992	0.9991	0.9989	0.9986	0.9982

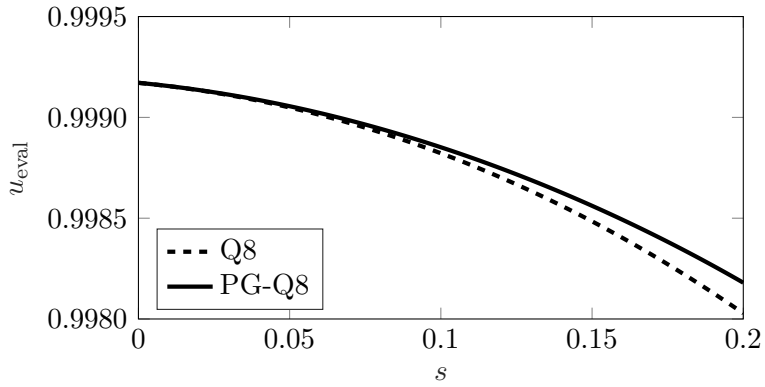

Figure 10: Illustration of the resulting radial displacement u_{eval} for the thick-walled cylinder example at $(r,\, z) = (R_i,\, 0)$ for different values of s. These values have been computed using $R_i = 1$ and $R_o = 2$.

Based on this example, it can be concluded that the Petrov-Galerkin formulation does not necessarily provide better results than the Bubnov-Galerkin formulation in all cases. Rather, it seems that for some problems, one element is more suitable, while for other problems, the other element is better. For a problem with an unknown displacement field, it does not seem possible to determine a priori which element formulation delivers better results.

5 CONCLUSION

In this work, an 8-node Petrov-Galerkin finite element formulation for the simulation of axisymmetric problems was presented and numerically investigated. The objective was to obtain a formulation that shows significantly lower sensitivity to meshes with distorted elements compared to the corresponding Bubnov-Galerkin formulation.

To achieve this, the core ideas of existing Petrov-Galerkin formulations for plane problems were utilized to develop an axisymmetric formulation. This includes the use of the common quadratic serendipity shape functions to approximate the virtual displacement field and the use of so-called metric shape functions to approximate the displacement field. The metric shape functions were defined based on skew coordinates.

The numerical results show that the developed formulation is capable of accurately reproducing quadratic displacement fields even when using meshes with highly distorted elements. In these cases, the Petrov-Galerkin formulation shows a superior behavior compared to the standard Bubnov-Galerkin formulation, which shows a significant decline in approximation accuracy. However, as demonstrated in the last example, when the displacement field is not quadratic, the Petrov-Galerkin formulation does not always demonstrate a less mesh-sensitive behavior compared to the corresponding Bubnov-Galerkin formulation.

6 4-NODE PETROV-GALERKIN FINITE ELEMENT FORMULATION

Finally, we would like to point out that we have also looked into the development of a 4-node Petrov-Galerkin finite element formulation for axisymmetric problems. We were hoping for a formulation that, like the 8-node element formulation described above, could accurately reproduce quadratic displacement fields even when using highly distorted meshes. This is possible for plane and three-dimensional problems, as shown, for example, by an element formulation based on the Enhanced Assumed Strain method [10]. However, it appears to be infeasible to transfer the procedure chosen therein to axisymmetric problems: The conventional Bubnov-Galerkin Enhanced Assumed Strain element formulations [6] are not capable of accurately reproducing quadratic displacement fields even when using regular meshes. Therefore, the development of a Petrov-Galerkin element formulation that achieves the stated objectives appears to be impossible from the outset; at least on the basis of the Enhanced Assumed Strain method.

7 ACKNOWLEDGEMENTS

We gratefully acknowledge the financial support provided by the Deutsche Forschungsgemeinschaft (DFG) – project number 466086399.

REFERENCES

[1] Lee NS, Bathe KJ. Effects of element distortions on the performance of isoparametric elements. *Int J Numer Methods Eng.* 1993;36:3553–3576. doi: 10.1002/nme.1620362009.

[2] Rajendran S, Liew KM. A novel unsymmetric 8-node plane element immune to mesh distortion under a quadratic displacement field. *Int J Numer Methods Eng.* 2003;58(11):1713–48. doi: 10.1002/nme.836.

[3] Xie Q, Sze KY, Zhou YX. Modified and Trefftz unsymmetric finite element models. *Int J Mech Mater Des.* 2016;12:53–70. doi: 10.1007/s10999-014-9289-3.

[4] Timoshenko S, Goodier JN. Theory of Elasticity. 2nd ed. New York: McGraw-Hill; 1951.

[5] Zienkiewicz OC, Taylor RL. The Finite Element Method: The Basis. Volume 1. 5th ed. Oxford: Butterworth-Heinemann; 2000.

[6] Simo JC, Rifai MS. A class of mixed assumed strain methods and the method of incompatible modes. *Int J Numer Methods Eng.* 1990;29:1595–1638. doi: 10.1002/nme.1620290802.

[7] Yuan KY, Huang YS, Pian THH. New strategy for assumed stresses for 4-node hybrid stress membrane element. *Int J Numer Methods Eng.* 1993;36:1747–1763. doi: 10.1002/nme.1620361009.

[8] Timoshenko S, Woinowsky-Krieger S. Theory of Plates and Shells. 2nd ed. New York: McGraw-Hill; 1959.

[9] Hampe E. Statik rotationssymmetrischer Flächentragwerke: Kreiszylinderschale. Band 2. 3rd ed. Berlin: VEB Verlag für Bauwesen; 1968.

[10] Pfefferkorn R, Betsch P. Mesh distortion insensitive and locking-free Petrov–Galerkin low-order EAS elements for linear elasticity. *Int J Numer Methods Eng.* 2021;122(23):6924–6954. doi: 10.1002/nme.6817.